Nuclear Instruments and Methods in Physics Research B 548 (2024) 165253

Contents lists available at ScienceDirect

Nuclear Inst. and Methods in Physics Research, B

journal homepage: www.elsevier.com/locate/nimb

Multi-Isotope determination of uranium-rich material using accelerator mass spectrometry

Adam M. Clark [a,*], Austin D. Nelson [a], Thomas L. Bailey [a], Drew Blankstein [a], Chevelle Boomershine [a], Gunnar M. Brown [a], Peter C. Burns [b,c], Scott Carmichael [a], Lauren K. Callahan [a], Jes Koros [a], Kevin Lee [a], Miriam Matney [a], Anthony M. Miller [a], Orlando Olivas-Gomez [a], Michael Paul [d], Richard Pardo [e], Fabio Rivero [a], Daniel Robertson [a], Ginger E. Sigmon [c], William W. von Seeger [a], Ed Stech [a], Regan Zite [a], Philippe Collon [a]

[a] Department of Physics and Astronomy, University of Notre Dame, Notre Dame, IN 46556, United States
[b] Department of Chemistry and Biochemistry, University of Notre Dame, Notre Dame, IN 46556, United States
[c] Department of Civil and Environmental Engineering and Earth Sciences, University of Notre Dame, Notre Dame, IN 46556, United States
[d] The Hebrew University of Jerusalem, Jerusalem 91904, Israel
[e] Argonne National Laboratory, Lemont, IL 60439, United States

ARTICLE INFO

Keywords:
Direct-AMS
Actinides
Multi-isotope survey
Nuclear forensics
Uranium ores
Uranium
Thorium
Protactinium

ABSTRACT

Environmental detection of trace isotopes ^{233}U and ^{236}U are important forensic signatures for identifying uranium ore materials or tracking anthropogenic releases from weapons fallout or nuclear reprocessing. Currently, Accelerator Mass Spectrometry (AMS) is the only method sensitive enough to detect signatures of ^{233}U/U and ^{236}U/U at the natural level due to the molecular interferences of ^{232}ThH and ^{235}UH, respectively, often present in conventional mass spectrometry. In this work, we detail the AMS capabilities of actinides developed at the University of Notre Dame's Nuclear Science Laboratory (NSL). For the first time in our laboratory, we have measured isotopic ratios of ^{236}U/U and explored additional signatures of ^{233}U and decay chain products ^{231}Pa and ^{230}Th in both natural ore material and two National Bureau of Standards samples. In this work we estimate a system sensitivity for ^{236}U/U of 1.4×10^{-11} and characterize the simultaneous detection of ^{233}U, ^{231}Pa, and ^{230}Th.

1. Introduction

The study of trace actinide isotope ratios within ore deposits provides insight into potential conditions of geological repository sites [1,2]. More specifically, ^{236}U/U signatures measured down to natural level (10^{-14} – 10^{-10}) that are a direct result of the neutron flux within the site [2]. Production of ^{236}U ($t_{1/2} = 23.42(4)$ Myr) [3] is dominated by neutron capture on ^{235}U ($t_{1/2} = 704(1)$ Myr) [4]. This production will be elevated in a high neutron flux environment and additional production channels are possible with fast neutrons via the (n, 3n) reaction. The detection of ^{236}U has been closely studied with accelerator mass spectrometry (AMS) as it is the only technique capable of measuring with a sensitivity that covers the aforementioned range of natural abundances [5].

Due to technological advances within AMS facilities, additional actinide isotopes down to ultra-trace levels have become accessible. For example, ^{233}U, which is anticipated as several orders of magnitude below that of ^{236}U, has been measured within water and air filter samples [6–8]. The production of ^{233}U ($t_{1/2} = 1.592(2) \times 10^5$ yrs) [9] requires either sufficient ^{232}Th content for neutron capture followed by the β^- decays of ^{233}Th and ^{233}Pa or fast neutrons for (n, 3n) reaction on ^{235}U. Since this differs from that of ^{236}U the combined ^{233}U/^{236}U signature is gaining traction for its use assisting with the identification of anthropogenic sources.

Within uranium ores, additional actinide isotopes accumulate because of the uranium decay chains. Work by Zhao et al. 2019 suggested that simultaneous detection of decay products using AMS may provide several unique signatures. For reprocessed materials, chemical treatment may remove isotopes with characteristic efficiencies [10]. Similarly, non-purified ore will accumulate well within the range of

* Corresponding author.
E-mail address: aclark11@alumni.nd.edu (A.M. Clark).

https://doi.org/10.1016/j.nimb.2024.165253
Received 4 October 2023; Received in revised form 26 December 2023; Accepted 16 January 2024
Available online 1 February 2024

decay counting or commercial mass spectrometry techniques and both $^{231}Pa/^{235}U$ and $^{230}Th/^{234}U$ ratios have been used for dating a variety of environmental materials [11,12]. The signature of a natural sample which has reached secular equilibrium will be observed with ratios of $^{231}Pa/^{235}U = 4.65 \times 10^{-5}$ and $^{230}Th/^{234}U = 0.307$. Suppression or elevation of these ratios which deviate compared to a known age would indicate the sample was not sufficiently isolated in the environment. In the case of nuclear forensic applications, the study of $^{231}Pa/^{235}U$ and $^{230}Th/^{234}U$ signatures have been used for dating of enriched uranium material since the time of chemical processing and may alternatively prove insightful as to the quality of the chemical purification. These previous studies required extensive chemical preparation to extract Pa and Th. For newly processed depleted material, these signatures are anticipated to be low enough that these techniques would require large sample sizes, making spectroscopic techniques unfeasible. Due to the high level of sensitivity of AMS, they could be added alongside ^{236}U and ^{233}U [10].

In this paper, we present the measurement procedure used for actinide detection, which has been used for the first time in our laboratory. Since no standardized material within the natural $^{236}U/U$ range of interest is commercially available, absolute measurements are reported and cross-referenced with material that has been measured at other facilities and two ^{235}U National Bureau of Standards (NBS) standard materials. We detail the development of our actinide AMS capabilities, stating our determined sensitivities for $^{233,\ 236}U/U$, $^{231}Pa/^{235}U$, and $^{230}Th/^{234}U$. To support our evaluations we compared our determined $^{236}U/U$ ratios with those previously measured and reported in literature and present values for materials for which, to our knowledge, have not yet been reported. Finally, we assess ^{231}Pa and ^{230}Th with what would be expected for natural material and the NBS standards.

2. Experimental methods

2.1. Sample selection and preparation

Most of the ore materials used in this study were selected from the Ewing collection housed at the University of Notre Dame. This collection is the largest collection of radioactive rocks and minerals in an academic setting in North America, with more than 1,300 individual specimens. Previously material from this collection has been studied using a variety of measurement techniques; however, this is the first study of these samples using AMS. Aside from location and mineral form, other information surrounding the sample collection process is unknown as many were collected decades ago. Additional samples used for validation of our procedure were sent to us from the Racah Institute of Physics at the Hebrew University of Jerusalem, some of which are believed to be the same material measured in Berkovits et al., 2000 [13].

Samples were prepared by acquiring loose powder or small fragments of the larger specimens. Only a few mg of each was used, and these were ground into a fine powder with a mortar and pestle to ensure uniformity of the material. Between samples, the mortar and pestle were cleaned with 5 M nitric acid and rinsed with isopropyl alcohol. They were then placed in a sonic cleaner for 15 min and then baked at 120 °C to drive off any remaining liquid. A portion of sample material was pressed directly into a 40-wheel vacuum-cleaned aluminum cathode purchased from National Electrostatic Corp. The rest of the sample material was mixed with varying amounts of 97.5 % aluminum powder purchased from Alfa Aesar at roughly 1:1 by volume. Aluminum is used as a binder material to assist with conductivity and fill volume to permit the use of small quantities of sample material in the cathode holders. Since the material has not been chemically treated, the sample material were present in a variety of mineral forms including uraninite (UO_{2+x}), boltwoodite ($(K,Na)(UO_2)(SiO_3OH)(H_2O)_{1.5}$, and clarkeite ($Na(UO_2)O(OH)n(H_2O)$). The processed material measured originated from the National Bureau of Standards, now the National Institute of Standards and Technology (NIST), and were in the form U_3O_8.

2.2. Instrumentation

A schematic of the relevant sections of the accelerator system are shown in Fig. 1. Negative molecular ions UO^-, PaO^-, and ThO^- were produced from a multi-cathode cesium sputtering source (MC-SNICS) built by National Electrostatics Corp. Energy filtration was performed immediately following the ion source with a 45° Electrostatic Analyzer, followed by a 90° injection magnet for mass selection prior to acceleration. Slits located at the entrance of the injection magnet were positioned at ±1 mm in the horizontal plane and ±3 mm in the vertical plane and, at the exit of the magnet, were ±0.5 mm in horizontal plane and ±3 mm in the vertical plane, resulting in a mass resolution of $M/\Delta M = 425$. A mass scan of two different samples is shown in Fig. 2 and demonstrates the variable compositions of the material. Beam currents of $^{238}U^{16}O^-$ were measured to be between 0.5 and 80 nA across the various sample materials. This selection of the single oxide molecular form is the most common selection for the actinides amongst AMS facilities, although fluoride molecules have been suggested as a possible solution towards combating ion source memory effects and ionizer poisoning [14].

Using a terminal voltage of 4.42 MV and selecting the 9 + charge state resulted in a beam energy of 43.9 MeV for ^{238}U, which was used as the initial tuning beam and as a reference point in which to scale the terminal voltage for other isotopes. These settings were a compromise between predicted charge state occupations, terminal voltage stability, and limitation of the maximum rigidity of the analyzing magnet (1.44 Tesla · m), which operated at 98 % of the maximum field. Despite successes of gas stripping at other facilities, foil stripping was found to be a more practical choice for our system. Even though gas stripping reduces angular straggling, our system currently lacks terminal recirculation, which means the stripping gas must exit by traversing the length of the acceleration tubes. As has been identified by other facilities and confirmed with internal observation, secondary stripping within the acceleration tubes caused by bad vacuum may introduce additional background. Neighboring isotopes will strip somewhere within the acceleration tube and acquire a wide range of energies. Some of the resultant energy and charge state combinations will match the rigidity required to reach the detector system [15]. The expense of the selection of carbon foil stripping was that frequent measurements of the transmission and occasional changing of foils were required due to foil degradation.

Following the analyzing magnet, a switching magnet steers the beam to the dedicated AMS beamline, described in Clark et al. 2023 [16]. On this beamline, a Wien Filter further suppresses neighboring contaminants and was found to suppress neighboring actinide isotopes by a factor of ~ 20 while operated at 95 % maximum field with vertical slits (positioned 4.1 m following the Wien Filter exit) with a slit gap of ± 1.5 mm. Demonstration of the suppression of the Wien Filter alone is shown in Fig. 3.

The final identification and detection of heavy-ions are performed using a combination of detectors which feature a Faraday cup, an ionization chamber detector, and time-of-flight system. Further details about the ionization chamber (IC) detector and time-of-flight system which uses two microchannel plate detectors can be found in Clark et al. 2023 [16].

2.3. Isotope identification

2.3.1. U-236 spectra

The identification of ^{236}U was supported through the comparison to simulation described in Clark et al. 2023 [16] and is shown in Fig. 4. It was found that the resolution provided by the IC was critical to discriminate additional contaminants of $^{209}Bi^{8+}$ and $^{186}W^{7+}$ which had times-of-flight between the neighboring U isotopes. These additional contaminants have not to our knowledge been discussed in literature, we believe the presence of these contaminants are due to the lack of

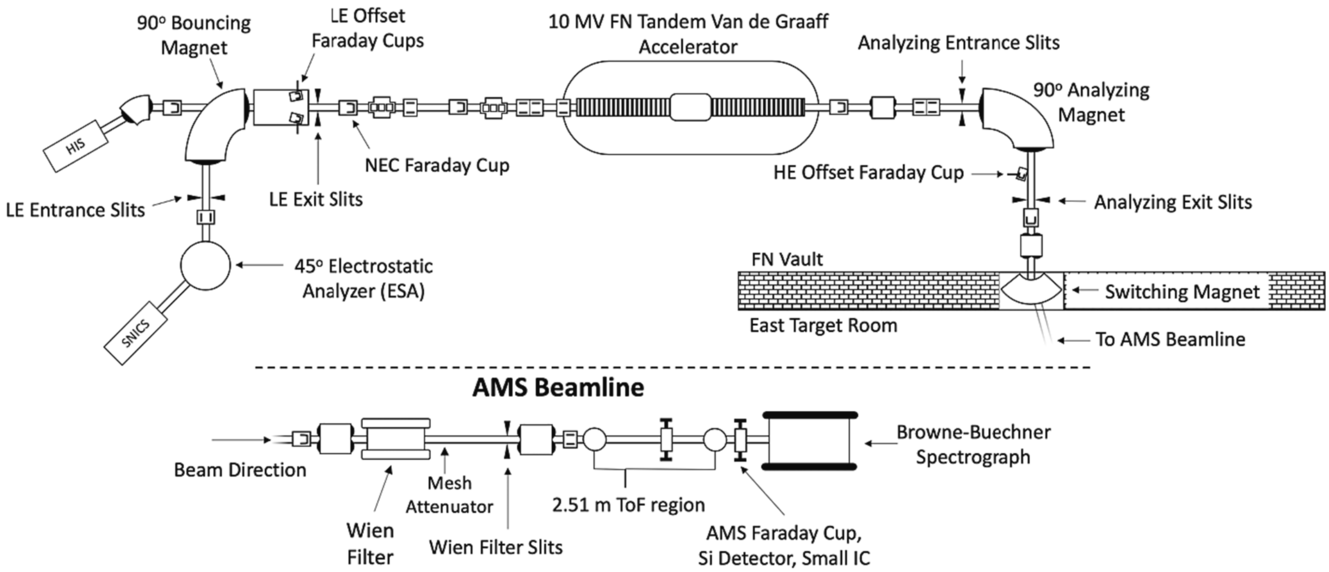

Fig. 1. Schematic layout of the system for AMS at the NSL. Negative ions are injected into the tandem and stripped with a selection of gas or a carbon foil. Positive ions are selected by the analyzing magnet and sent down the beamline dedicated for AMS for further filtration and detection from either the time-of-flight system for heavy ions or the Browne-Buechner spectrograph operated in gas-filled mode for isobaric discrimination. See Section 2 for more information.

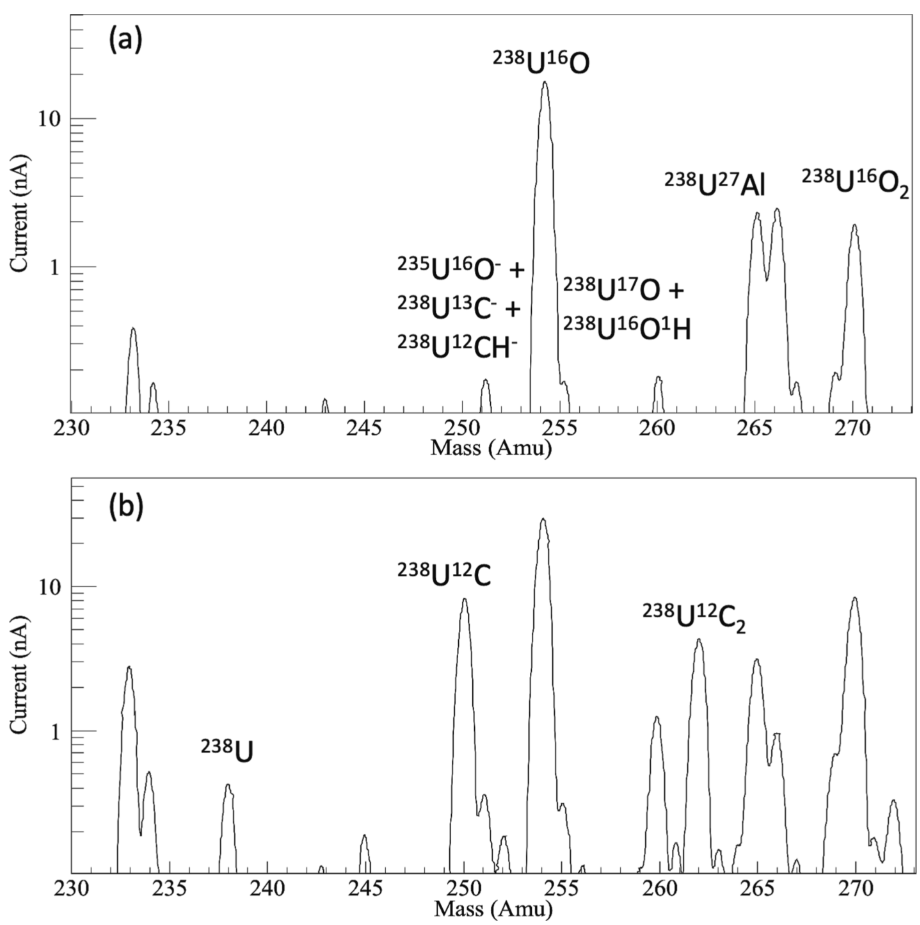

Fig. 2. Mass scans recording the current following the injection magnet are shown. Spectra (a) is for a sample from Rabbit Lake, Sask., Canada and (b) is from the Oklo reactor site Zone 9 in Gabon, Africa to demonstrate the varied composition of non-treated material within the mass range of interest for UO^- injection. Some, but not all, peaks have been identified which are suspected to contain measurable quantities of major uranium isotopes.

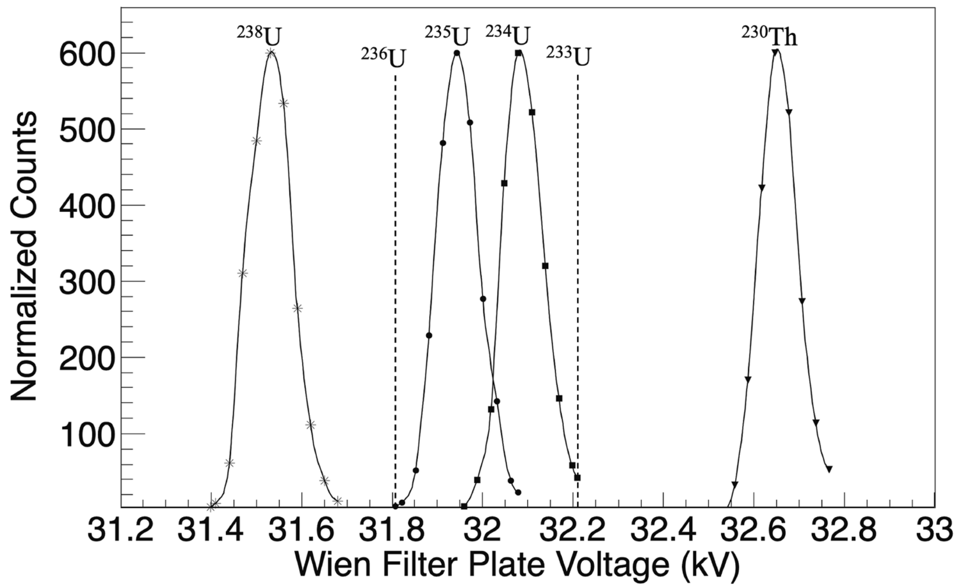

Fig. 3. The superposition of scans with normalized intensities shown for $^{234,\ 235,\ \text{and}\ 238}$U and ^{230}Th with only the Wien Filter voltage varied. The projected peak positions for ^{236}U and ^{233}U are shown. The suppression factor of the neighboring isotope one mass unit below as determined by the ^{235}U rate at the ^{236}U voltage is 124 and the FWHM of the distributions indicate a M/Δ M of 305 for the Wien Filter alone.

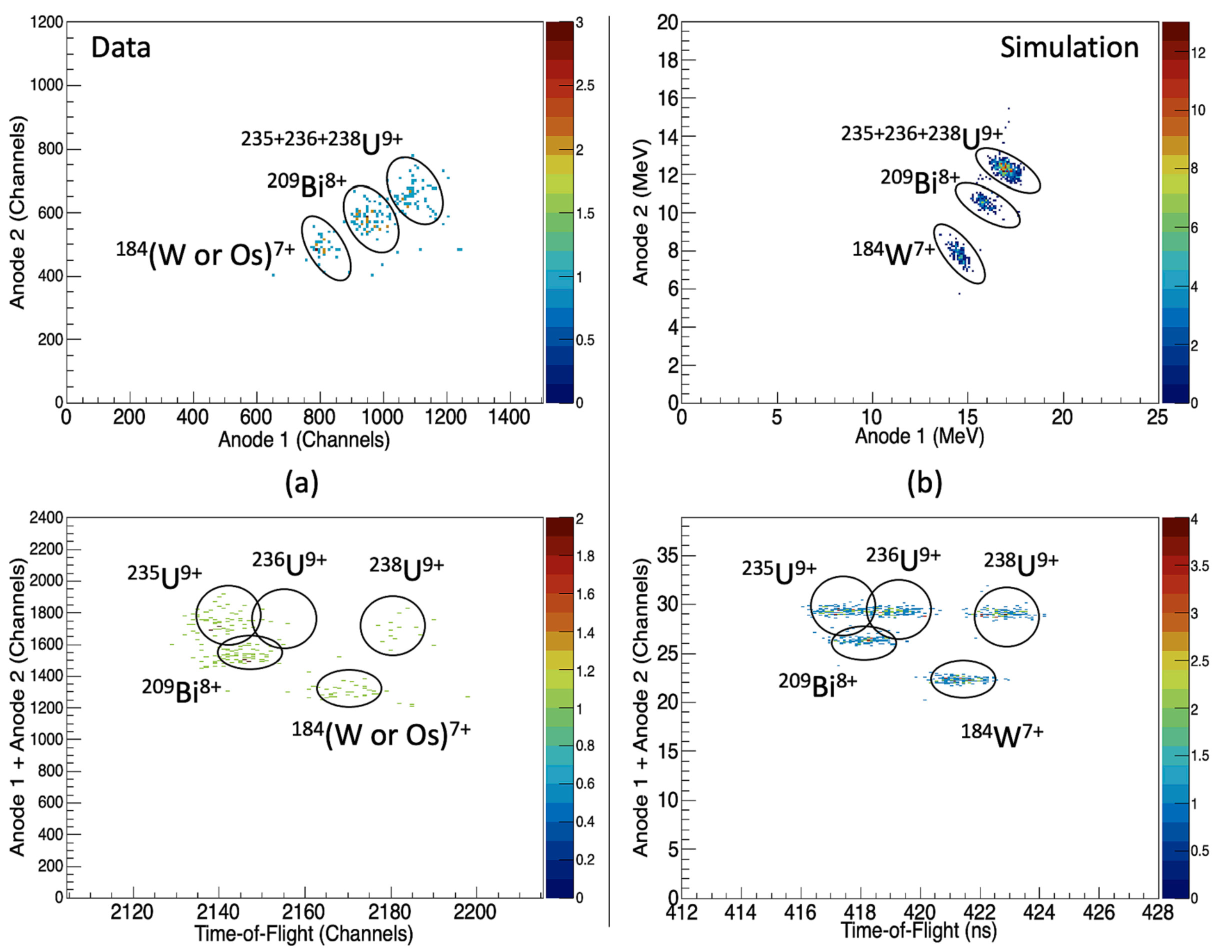

Fig. 4. Experimental and simulated spectra for the mass 236. Spectra (a) show a 1.5 hr run from sample Ewing 508: Rabbit Lake with contaminant identifications and regions. In contrast, (b) shows a simulated spectra using a GEANT4 simulation. The identification of the simulated ions are labeled and demonstrate good agreement with the data.

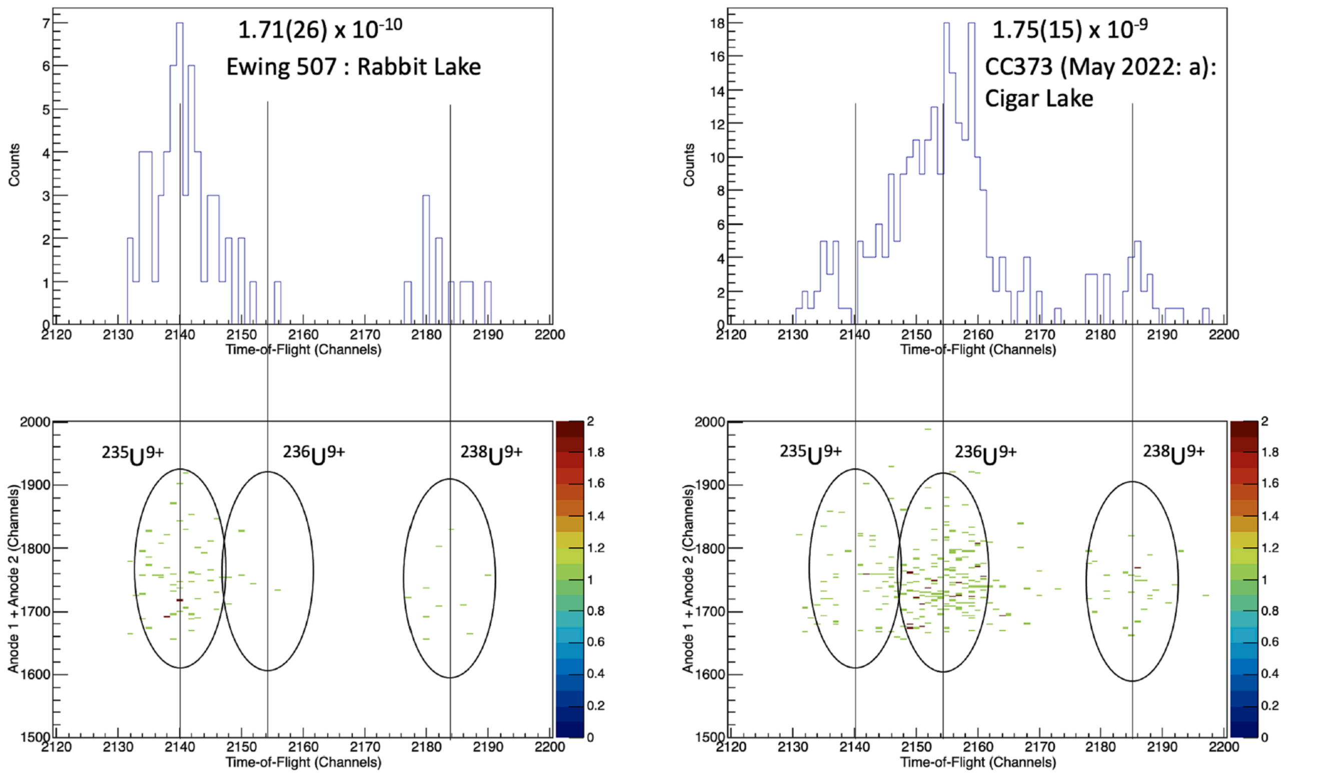

Fig. 5. Two example spectra from a subset of data collected for Ewing:453 and CC373 samples with an energy software cut applied using IC energy loss information. The identification of the particles remaining are shown and the counts attributable to ^{236}U can be identified with the time-of-flight information. Regions have been circled here to guide the eye to anticipated energy and time-of-flight regions for each isotope of interest, but they do not explicitly represent the regions of interest used for analysis.

chemical purification of the sample materials. Yet, due to the energy resolution of the detector system they were determined not to interfere with our measurements. Spectra gated by energy are shown in Fig. 5 and demonstrate the final spectra used for isotope ratio determinations.

2.3.2. Additional actinide isotopes

Additional isotopes ^{233}U (see Fig. 6), ^{231}Pa (see Fig. 7), and ^{230}Th (see Fig. 8) were explored for this work. In each case, time-of-flight versus energy spectra demonstrate our capabilities and highlight the importance of refining the various slits along the system to optimize the mass resolution of each filtering element.

2.4. Measurement procedure

Due to variable ion source currents, as well as the total particle transmission through the accelerator system (0.04–0.06 % as measured from the NEC Faraday cup to the AMS Faraday cup), ^{238}U^{9+} currents measured at the end of the beamline were typically less than 200 electrical picoAmperes. In order to reduce measurement uncertainties resulting from these currents, the method of measuring with respect to an attenuated ^{235}U beam was adopted. The stability and accuracy of this method was determined through periodic measurements of the ^{235}U/^{234}U isotope ratio. The attenuation factor of a mesh attenuator positioned at the exit of the Wien Filter was determined by comparing detector rates with and without the mesh attenuator. Beam intensity was reduced to rates safe for the detector system prior to acceleration. Since the attenuation factor can often depend on the beam tune, the attenuation factor was remeasured following any change to the focusing elements. The result was found to be a factor of 136 ± 5 reduction in beam rate.

The measurement procedure required periodic switching between several masses of interest. For each sample material, transmission measurements using ^{238}U were performed at the beginning and end of the measurement cycle, followed by 5 minute measurements of the attenuated ^{235}U and non-attenuated ^{234}U. The ^{235}U/^{234}U ratio served both as a confirmation that the material reflected natural concentrations and to monitor for system stability. Next, a longer counting sequence of the rare isotopes was performed, 3 hours for ^{236}U broken up into runs of, at most, 30 minutes, and ended with re-measurements of ^{235}U and ^{234}U. The sequence either followed by another long measurement of a trace isotope of interest or ended with a final transmission measurement depending on the counting statistics or ion source output. During each run, ^{238}U was recorded on an offset Faraday cup on the low-energy side due to the jumping capabilities of the injection magnet bias voltage.

Switching between isotopes on our system requires several minutes to change the injection system, terminal voltage, Wien Filter voltage, and insert the proper attenuation and/or measurement system manually on the beamline. To avoid hysteresis within magnetic elements along the system, only electrostatic elements are scaled for each mass. These settings are first determined through calculation and then optimized by maximizing count rates within regions of interest on the detector system.

In addition to measurements of ^{236}U isotopic ratios, additional long-lived isotopes of ^{233}U, which provides a strong indication of reprocessing activities, as well as ^{230}Th and ^{231}Pa were explored using the same procedure.

2.5. Isotopic ratio determinations

The determination of isotopic ratios for this study deviated from what is commonplace for most studied AMS isotopes. First, there was no true blank material that could be used for simplistic background corrections. The subtraction of background instead was performed through fits of the neighboring contaminant when possible. All remaining counts within the region of interested had to be regarded as true events.

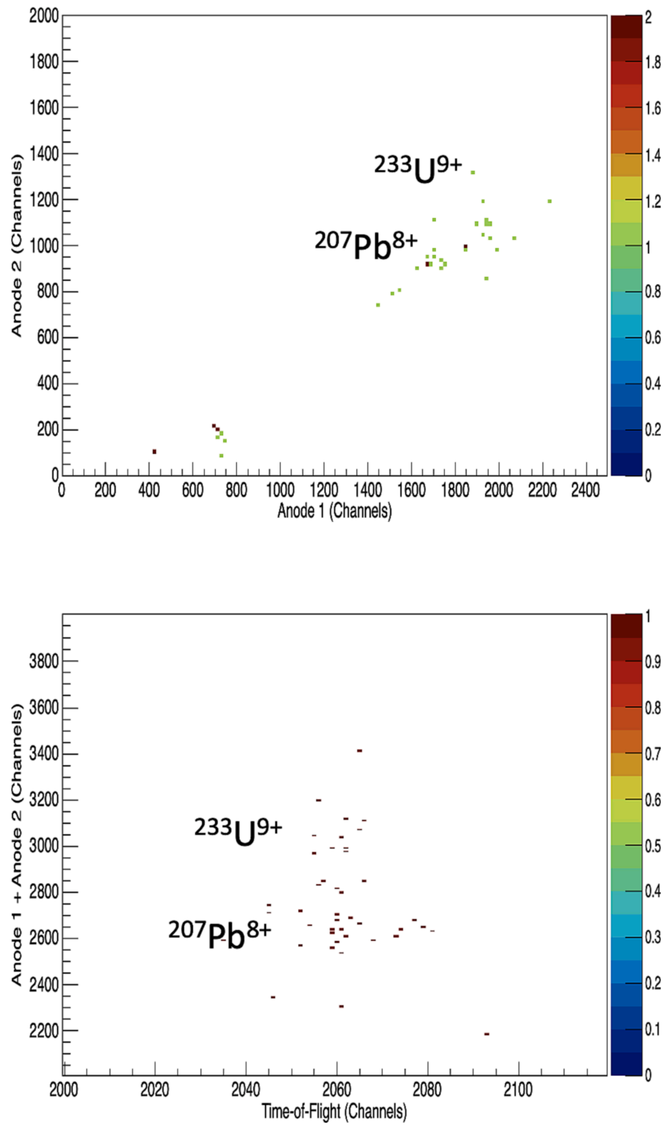

Fig. 6. Spectra for mass 233. The top spectrum shows energy loss information from the two anodes of the IC, while the bottom spectrum shows the summed energy vs the time-of-flight. The data in these spectra are a sum of runs taken for an ore sample and a purified uranium sample found to be elevated in ^{233}U. The ore material contributed contamination identified as $^{207}Pb^{8+}$. The channels for energy and time-of-flight differ from other figures in this section due to differences in detector settings.

Additionally, an in-house calibration series was not produced as the chemistry procedures are not yet established within our laboratory. Therefore, the measurements of unprocessed material and their reported values serve as our point of comparison. The determination of the concentration was performed via the following expression

$$\frac{Trace}{U_{total}} = \frac{Trace}{^{235}U}\left(\frac{^{235}U}{U_{total}}\right)_{natural}$$
$$= \frac{N_{trace}}{A \times N_{235}}\,\frac{t_{235}}{t_{trace}}\,\frac{I_{235}}{I_{trace}}\,\frac{\varepsilon_{235}}{\varepsilon_{trace}}\left(\frac{^{235}U}{U_{total}}\right)_{natural},$$

where *Trace* refers to the trace isotope being measured, U_{total} is the total uranium content, ^{235}U is the ^{235}U content, N is the number of counts of the trace isotope or ^{235}U, t is the counting time for the trace or ^{235}U measurement, I is the averaged ^{238}U current measured on the offset cup labeled as recorded during either the ^{235}U or trace isotope run, ε is the efficiency for detection of ^{235}U and the trace isotope, which incorporates electronic deadtime and transmission through the detection system, and A is the attenuation factor of the mesh attenuator.

An assessment of $^{235}U/^{234}U$ was used as both a diagnostic tool of the accelerator system stability and a verification method to determine if the sample material composition was consistent with expected natural abundances. A plot of the determined $^{235}U/^{234}U$ ratios for each sample is shown in Fig. 9. These ratios are shown with a comparison to 'natural' abundances for $^{235}U/U$ (0.7204(6)%) [4] and $^{234}U/U$ (0.0054(5)%) [17] as reported in literature which suggest a $^{235}U/^{234}U$ ratios = 133 ± 12. It was found that the majority of the samples from this study were within good agreement to this ratio with notable exceptions being the Oklo samples and U-005 material. In the case of the Oklo material, it was anticipated that the ^{234}U concentration would be in secular equilibrium; however, the depletion of ^{235}U for these samples were not known.

For the U-005 sample it is known that the ^{235}U level is depleted and these values were compared to the certified values. The determined $^{235}U/^{234}U$ ratio of 230 ± 12 was within good agreement of the expected value of 225 ± 4 using its reference certificate [18].

2.6. *Cross-talk background*

In order to support validity of low statistics measurements, we investigated the possibility of background contamination due to the binder material and cross-talk within the ion source between samples. Measurements of samples of Al powder used as a binder yielded no background counts within the mass 236. Additionally, no observable discrepancy was found for measurements of uranium samples with and without the binding Al. To explore cross-talk, pure Al was sputtered immediately following measurement of a uranium sample. It was found that $^{238}UO^-$ current remained measurable (several nA initially) on the low energy Faraday cup for several minutes before falling below detection levels due to "ion source memory". When sending mass 238 to the detector system, it was observed that the detectable ^{238}U beam intensity continued to decrease before reaching a plateau of ∼ 300 counts/s after ∼ 1 hr of sputtering. Therefore, in order to reduce cross-talk between samples, each sample was sputtered for 1 hr prior to using data for analysis. Using this condition, we calculated that given the observed background rate of ^{238}U on the detector the isotopic ratio within the aluminum powder or from the ion source cross-talk need to be on the order of $^{236}U/U \sim 10^{-3}$ to elevate a sample measurement (which is unlikely).

A similar study was not performed to determine binder contributions to ^{230}Th or ^{231}Pa, but should be re-visited if further determinations of these isotopes are pursued. However, the measurements of the NBS standards indicate that the background level is no more than the lowest recorded values, and we calculate that the levels obtained are consistent with the expected orders of magnitude given the NBS sample ages, although it is acknowledged that these measurements have large, attributed uncertainties.

3. Sensitivity determination

Since no 'blank' ^{236}U material exists, indirect determination methods through 239/238 mass ratio [19,20], or through Gaussian fitting and subtraction of contaminating ^{235}U [21,22] are used to estimate system sensitivities. In this work, since we elected not to chemically process material, a sample known to be void of mass 239 was not available. Additionally, we found that an intense low-energy contaminant prevented a determination due to a similar time-of-flight and pile-up within the IC. Therefore, we systematically explored the suppression of the ^{235}U current from the injection system, accelerator, Wien Filter, and the detection system. The resultant suppression factors are given in Table 1. From these factors we determine that the suppression of the accelerator system alone was estimated to allow for measurement of $^{236}U/U = 5.9 \times 10^{-10}$. This, of course, is dependant on the level of the $^{235}UH^-$ formation

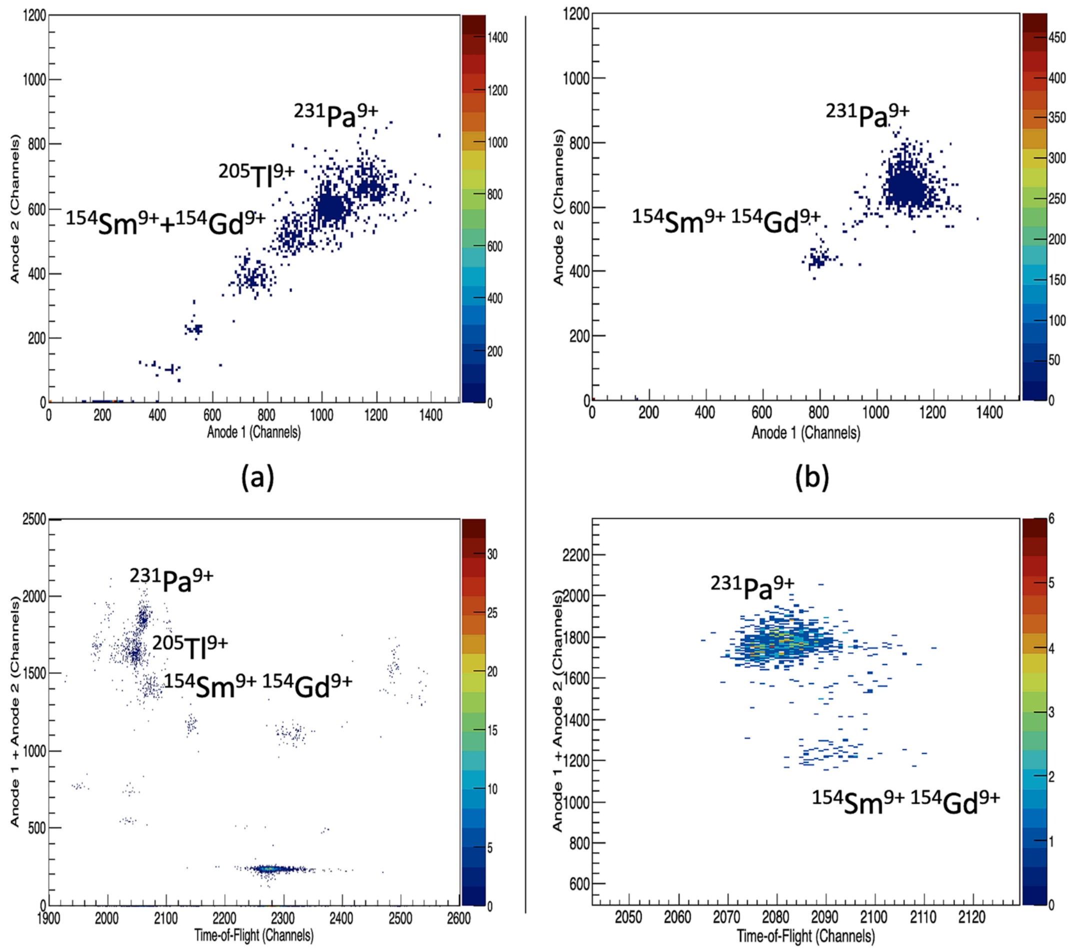

Fig. 7. Spectra at settings for mass 231. (a) Shows a 5 min run from sample Ewing 508: Rabbit Lake while the system slits are wide open for tuning. In contrast, (b) shows 15 min of the Ewing 692: Oklo Zn. 9 sample with the slits in their final positions as described in the text.

from the ion source. An additional factor of 75 was determined when using the detector system to remove ions well outside of the region of interest in energy and/or time-of-flight as the targeted ions. The resultant estimate of the overall system sensitivity is $^{236}U/U = 1.4 \times 10^{-11}$. This could be improved further with more restrictive cuts on the regions of interest or improvements to the detector system's resolution but was estimated to be adequate for the samples studied.

4. Results and discussion

4.1. U-236 determinations

The determined values for the isotopic ratios from this study are presented in Table 2 where uncertainties have been fully propagated to include other contributions beyond counting statistics. In cases where multiple independent measurements were possible, the listed uncertainty is either the error on the mean given by the standard deviation over the root of the number of measurements or the propagated uncertainty on the average, where the larger of the two was chosen. Validation of these values for $^{236}U/U$ was performed through the measurement of uranium materials originating from previously measured locations, specifically Rabbit Lake ($1.12 \pm 0.06 \times 10^{-10}$) [23], Cigar Lake ($3.3 \pm 0.5 \times 10^{-10}$ [13], $5.6 \pm 1.5 \times 10^{-10}$) [24], Great Bear Lake ($6.2 \pm 2.2 \times 10^{-10}$) [25], a depleted uranium NBS standard U-005 ($4.66 \pm 0.05 \times 10^{-5}$)) [18], and a "natural uranium" NBS standard ($8.2 \pm 0.6 \times 10^{-6}$) [13]. It was found that our results for these materials were in good agreement with these evaluations at other facilities and our Cigar Lake value favored the more recent measurement. A plot of the evaluated isotopic ratio compared to values found in literature are presented in Fig. 10.

The largest deviations followed from sample materials CC373, CC374, and Great Bear Lake. CC373 was believed to be the material used in the Berkovits et al. 2000 [13] study and CC374 was to be the same material but stored in separate vials. For this material, the Berkovits results were not reproduced and suggested sample contamination. It is possible that during the past 22 years of storage, which was near both the 950b and U-005 material, that cross-contamination occurred. Measurable contamination at this low level is easy and further demonstrated by an isolated sample of the CC373 measured which was believed to be contaminated from a mortar and pestle used for actinide target production performed in our laboratory. Although the source of contamination cannot be known for certain, if it came from either U-005 or 950b then it would only take on the order of 0.1 mg to raise a 5 g sample of Cigar Lake material by one order of magnitude while having a negligible effect on the other ratios measured. In a report from Fields et al. 1976, it was even suggested that contamination was observed due to trace levels of airborne uranium which was measured to contain $^{236}U/U$ content on the order of 10^{-6} [26].

Similarly, the Great Bear Lake sample was measured lower than what has been reported in literature. In Rokop et al. 1971 [25], the material was described as processed ore. It is further described as being undocumented and identified only as from Port Hope and was "probably mined as pitchblende at Great Bear Lake". Whether the material was elevated from cross-contamination, was irradiated, or was from another place of origin is unclear.

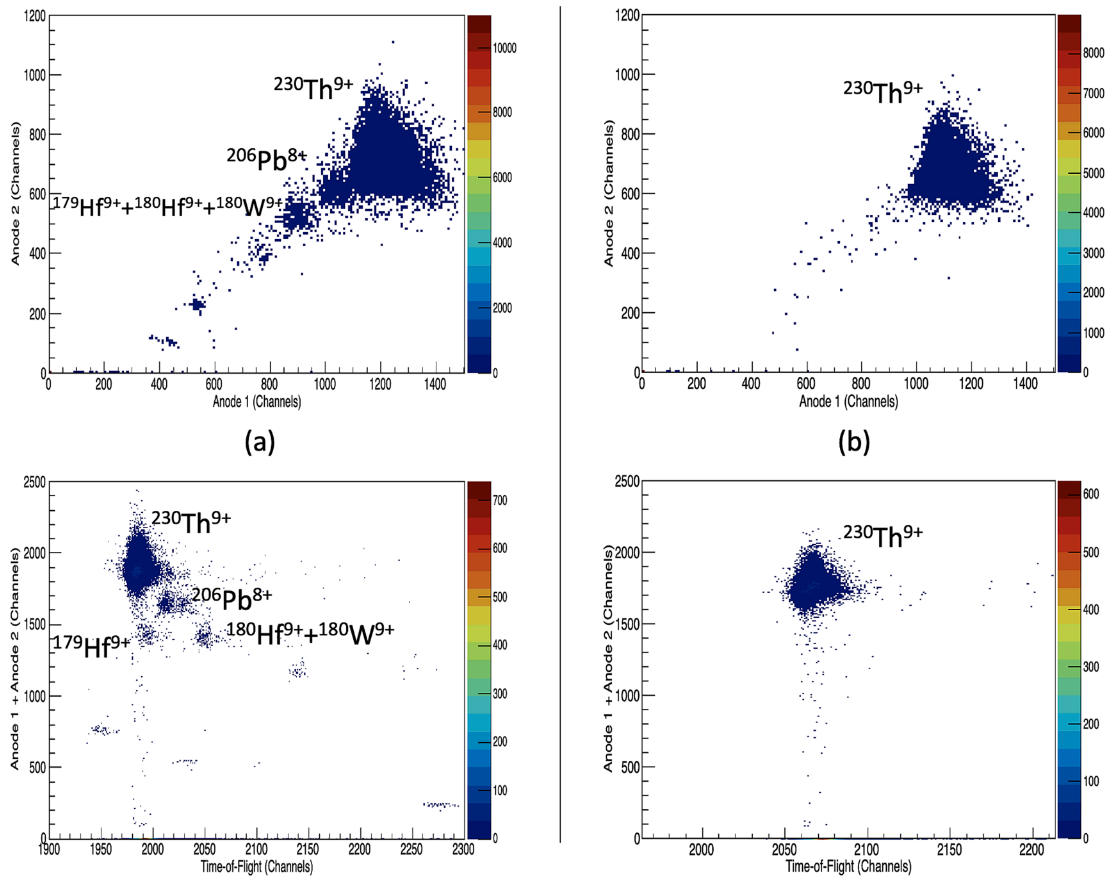

Fig. 8. Spectra at settings for mass 230. (a) Shows a 5 min run from sample Ewing 508: Rabbit Lake while the system slits are wide open for tuning. In contrast, (b) shows 15 min of the Ewing 692: Oklo Zn. 9 sample with the slits in their final positions as described in the text.

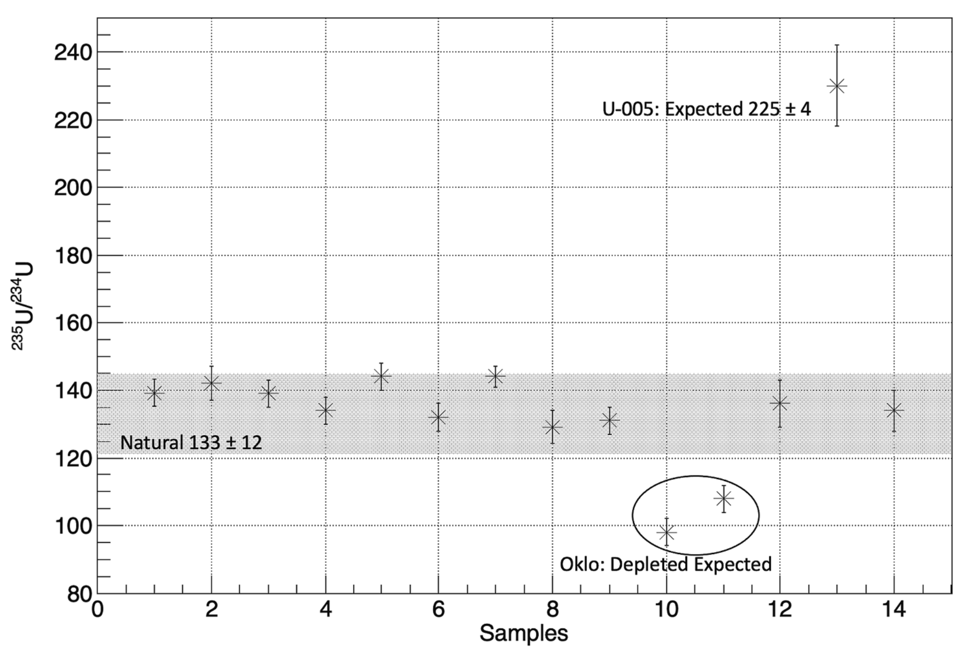

Fig. 9. The ratios for each sample demonstrate good agreement for ore samples which were anticipated as containing natural concentrations of the three primary uranium isotopes. Sample U-005 was consistent with its certificate value and the Oklo samples were consistent with being depleted in ^{235}U.

Table 1
Estimated suppression factors of various system components were determined through systematic comparison of rates comparing the settings for ^{235}U and ^{236}U.

System Component(s)	Est. Suppression Factor
Injection System	173
Terminal Voltage	565
Wien Filter	124
Accelerator System (Total)	1.21×10^7
Detection System	41
Total	5×10^8

The largest contributor to the uncertainty of the measured isotopic ratios was the statistical uncertainty. Due to the beam current output, accelerator transmission, and low ^{236}U content, the count rate on the detector was limited.

4.2. Pa-231 and Th-230 dating exploration

The use of the high sensitivity and simplified sample preparation provided by AMS may allow for more sensitive applications of radioisotope dating with ^{231}Pa and ^{230}Th. In natural materials where these levels have reached high isotopic ratios, current dating techniques of alpha spectroscopy or commercial mass spectrometry are sufficient. However, as inventories of processed uranium materials have aged since the beginning of the atomic age, the application of this dating technique could provide insight into when the uranium was last processed. This technique has been explored in several studies of enriched ^{235}U materials [27–29].

In order to explore the feasibility of multi-isotope determinations with our system, the electrostatic and magnetic elements were scaled to measure ^{231}Pa and ^{230}Th. The results are presented in Table 2 and shown in Fig. 11. As noted previously by Zhao et al. 2019, cross element AMS determinations are difficult to assess and, in many cases, should be viewed as neither precise nor accurate [10]. Reference materials to determine ionization efficiencies within the ion source were not available for this study. However, it may be expected that the behavior will follow measurements with similar ion sources. Therefore, the presented values have been corrected for ionization efficiency using results from Fifield 1997 [30] and Christl et al. 2007 [31]. The relative ionization efficiencies for XO^- formation were reported to be 2.87 ± 0.33 for U/Th and 2.15 ± 0.20 for U/Pa from these two studies respectively. Using these values, we aimed to assess observations of relative differences between the samples and compare with the expected secular equilibrium of natural materials.

It was found that the levels for the natural material fall within agreement of secular equilibrium for the ore material and were much lower for the NBS standard material due to chemical purification. The content of $^{231}Pa/^{235}U$ for the NBS material was found within the correct order of magnitude corresponding to the listed ages for the material but improved statistics are required as only a single count was observed for each sample. This was not true for ^{230}Th as the level for sample 950b was higher than expected by several orders of magnitude. Follow-up measurements would be required to improve the statistics; however, it is not expected to be the result of "memory effects" due to the high levels from the ore materials since 950b was measured directly after measuring U-005, which was found to be lower in $^{230}Th/^{234}U$. The uncertainty values presented in this exploration are large relative to other techniques even for the ore samples. In this case, the largest contribution to the uncertainties is from the ionization efficiency corrections that were used. In future studies, cross-elemental standards must be produced, however, consistency compared to untreated material would need to be proven. Discussion by Zhao et al. for fluoride investigations suggest that this may not be a trivial task as a major limitation may be consistency of the ionization efficiencies from various sample materials [14]. It is clear, however, that had the samples been chemically treated for uranium measurements, these signatures would have been lost altogether.

5. Conclusion and outlook

Measurements of the uranium series for natural ore samples and elevated material provided a test of the newly developed actinide AMS capabilities at the NSL. Isotopic ratios for samples were consistent with values reported at other facilities for ores originating from select loca-

Table 2
Measurements of measured isotopic ratios in both ore samples and processed uranium material. Uncertainties (1 sigma) are listed either as fully propagated including both statistical and experimental components or, if multiple measurements were made, as the error on the mean (whichever was larger). The presented values for ^{231}Pa and ^{230}Th have been corrected for ionization efficiencies within the ion source. Instances where uncertainties appear disproportionately large are the result of low statistics either from the observed ratio or low ion source current (<0.5nA).

Sample	Description	$^{235}U/^{234}U$	$^{233}U/U$	$^{236}U/U$	$^{231}Pa/^{235}U$	$^{230}Th/^{234}U$
Natural Material						
Ewing:453	Clarkeite: Spruce Pine, NC, US.	139(4)	4.8(4.8)E-10	1.23(44)E-10	4.55(76)E-5	0.397(47)
Ewing:507	Uraninite: Mi Vida, Mine, UT, US	142(5)	N.A.	1.52(42)E-10	2.52(22)E-5	0.404(52)
Ewing:508	Boltwoodite: Rabbit Lake, Sask., Canada	139(4)	N.A.	1.71(26)E-10	3.14(76)E-5	0.427(50)
Ewing:651	Uraninite: Cigar Lake. Sask., Canada	134(4)	1.9(1.9)E-11	2.78(75)E-10	4.39(43)E-5	0.400(47)
*CC373 (1st exp.)	Uraninite: Cigar Lake Sask., Canada	144(3)	1.0(1.0)E-11	1.74(31)E-9	6.77(56)E-5	0.467(57)
*CC373 (follow-up exp.)	Uraninite: Cigar Lake Sask., Canada	129(5)	N.A.	1.75(15)E-9	5.29(58)E-5	0.397(57)
*CC374	Uraninite: Cigar Lake Sask., Canada	131(4)	N.A.	1.81(20)E-9	3.89(21)E-5	0.441(63)
Ewing:UNM-M-0907	Uraninite: Great Bear Lake, NWT, Canada	133(6)	N.A.	1.43(61)E-10	5.1(1.8)E-5	0.521(96)
Ewing:692	Oklo Zone 9 Gabon, Africa	98(4)	N.A.	1.66(55)E-10	5.94(29)E-5	0.470(55)
Ewing:707	Oklo Zone 10 Gabon, Africa	108(4)	N.A.	2.1(1.0)E-9	7.0(2.6)E-5	0.644(94)
NDUNM 2	Silica-rich Sediment: Laguna, NM, US	136(7)	N.A.	5.8(5.8)E-9	5.3(1.1)E-5	0.759(95)
Processed Material						
U-005	NBS Material (1971)	230(12)	<6.0E-11	4.83(32)E-5	3.4(3.4)E-8	0.00011(6)
950b	NBS Material (1978)	134(6)	1.92(45)E-9	9.2(5)E-6	2.2(2.2)E-8	0.0024(4)

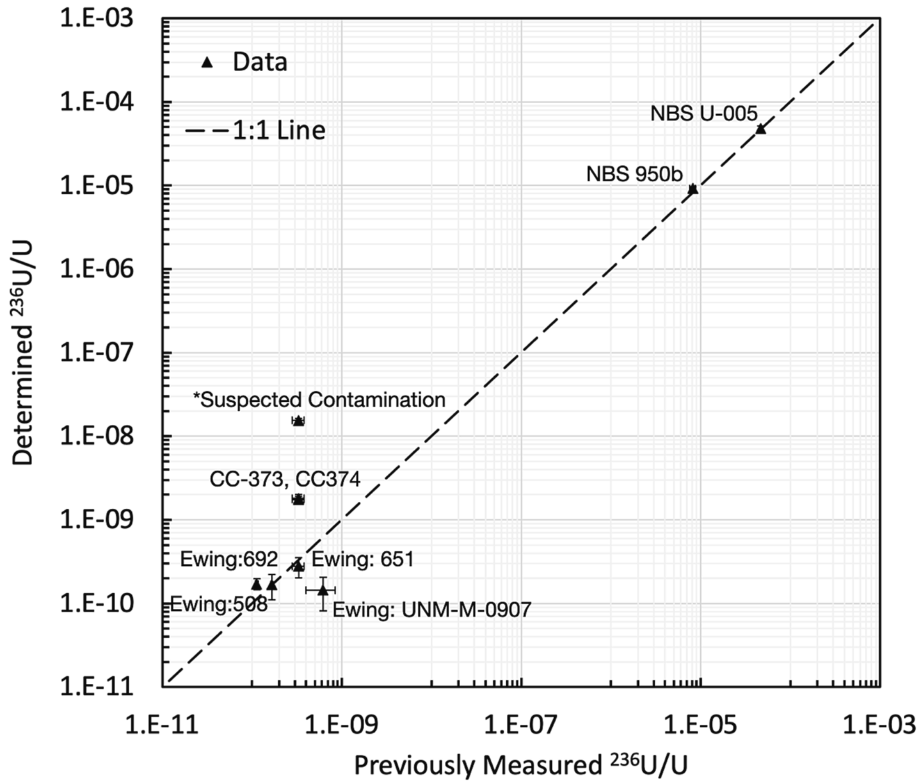

Fig. 10. Determined values for ^{236}U/U are plotted against values which can be found in literature. Good agreement can be seen compared to a 1:1 line with exceptions being expected as the result of cross contamination in our laboratory or during storage. The values which disagree, namely the CC373, CC374, and Great Bear Lake are suspected to be the result of cross-contamination and/or misidentification and are discussed in the text.

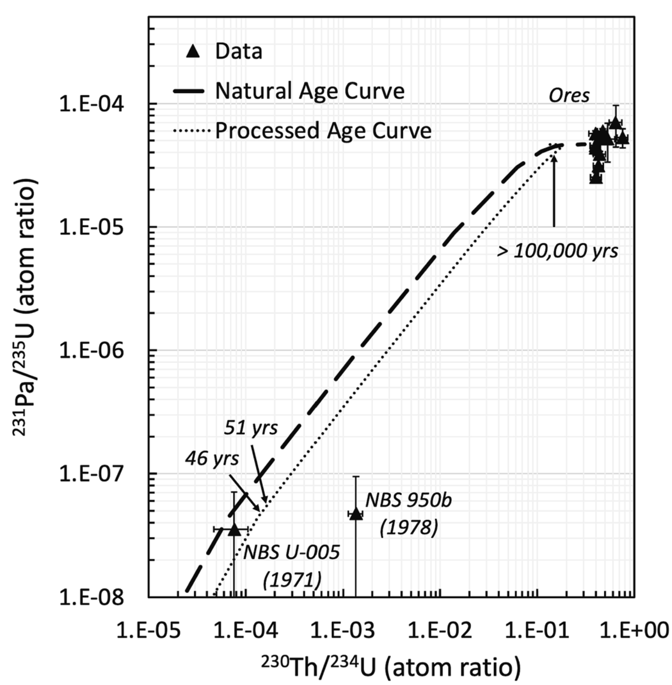

Fig. 11. Corrected values for ^{231}Pa and ^{230}Th determinations are plotted and compared with expected values for the age curve from build-in due to natural decay of uranium. Both age curves determine ^{231}Pa/^{235}U levels from the decay of $^{235}\text{U} \rightarrow {}^{231}\text{Th} \rightarrow {}^{231}\text{Pa}$, however the "Natural Age Curve" determines $^{230}\text{Th} \rightarrow {}^{234}\text{U}$ levels from $^{238}\text{U} \rightarrow {}^{234}\text{Th} \rightarrow {}^{234}\text{U} \rightarrow {}^{230}\text{Th}$ while the processed Age curve only considers $^{234}\text{U} \rightarrow {}^{230}\text{Th}$ decay. Years 46 and 51 are indicated on the processed age curve corresponding to the known ages of the NBS materials.

tions. During this measurement campaign, the lowest determined ^{236}U/U isotopic ratio was found to be $1.23(44) \times 10^{-10}$. For practical purposes, we assess this to be our current sensitivity limit. Recalling that the range of natural material was estimated to be 10^{-14}–10^{-10}, our system has now been demonstrated to be capable for measurements at the high end of this natural range and is well suited to detect material elevated in ^{236}U. However, when projecting from the measurements of the suppression factors for ^{235}U we estimate that a lower limit of $\sim 1.4 \times 10^{-11}$ may be achievable. At present we are limited by ion source output, accelerator transmission, detection efficiencies, and the possession of known low-level sample material. Still, we have successfully laid the groundwork for uranium-specific studies to be performed in the future, with improvements of the system efficiency underway. In addition to ^{236}U, the presented scaling method and detector system was demonstrated to allow for the detection of other actinide isotopes within a single sample.

The omission of chemical processing of the uranium-rich sample materials allowed for simultaneous detection of other naturally occurring actinides, which may provide an additional distinguishing signature at the cost of consistency in output from the ion source. This could serve as a critical screening method for several signatures before more sensitive studies are conducted. When higher sensitive measurements are desired, smaller sample sizes are used, or material with low uranium content are to be measured, chemical preparation well established by other facilities will be implemented for future studies. Despite no explicit normalization procedure for cross-element measurements in this experiment, it provides further indication that additional actinides could be measured with this method to obtain a more detailed forensic signature. With our demonstrated capabilities, we were able to obtain ^{231}Pa/^{235}U and ^{230}Th/^{234}U values from a few mg of a depleted uranium sample on the order consistent with an age of 53 yrs since the samples were created. Again, upgrades to both the scaling procedure to reduce measurement times, increase system efficiency, and efforts to implement a reliable method of normalizing cross-elemental samples will be required to achieve sufficient statistics and greatly reduce uncertainties before dating could be considered reliable.

With the presented procedure, measurements were made relative to $^{234,\,235}$U instead of ^{238}U. This allowed us to overcome the higher uncertainty inherent to sub-200 pA current measurements on the last beamline Faraday cup. This method works well for material within a few percent of natural abundances. In the instances where this isotopic ratio deviates, however, the picture was more complex. Until higher beam currents are achieved, further improvement of uncertainties and verification of deviations in the observed ^{235}U/^{234}U ratios will require an independent verification using an additional measurement technique.

Future explorations with these capabilities must resolve how cross-elemental normalization will be performed. Either compatible spike material will need to be selected on a case-by-case basis or a method of normalization with other techniques, such as alpha spectroscopy or gamma spectroscopy, will be necessary. If a reliable cross-elemental correction is obtainable with sufficient uncertainties, and higher efficiencies can be obtained with our system, the prospect is that sub-milligram amounts of depleted or even natural samples could be measured for age-determination with no chemical preparation. This would be a major improvement over techniques limited to large chemical reductions to obtain enough material for measurement.

The capabilities demonstrated through this work were encouraging first results for our laboratory. We believe improvements to the efficiency for uranium measurements, namely standardized chemical preparation, as well as improvements to the detector system may result in an increase in a factor of 10 or more. Further improvements will require more drastic changes such as the selection of a different charge state to improve occupancy, or major upgrades to the gas stripping mechanism and analyzing magnet. For more drastic improvements to the range relevant for astrophysical ^{244}Pu detection it is likely that a new, smaller system would be required. Encouraging results on machines as small as 300 kV have been demonstrated at other facilities [32,33]. Yet, capabilities developed over the last several years in our laboratory allow for future assessment of some natural ore material to include ^{36}Cl, ^{41}Ca, ^{129}I, and the actinides all on one system.

CRediT authorship contribution statement

Adam M. Clark: Conceptualization, Formal analysis, Investigation, Methodology, Software, Validation, Visualization, Writing – original draft. **Austin D. Nelson:** Conceptualization, Investigation, Methodology, Validation, Writing – review & editing. **Thomas L. Bailey:** Investigation, Methodology, Validation, Writing – review & editing. **Drew Blankstein:** Investigation. **Chevelle Boomershine:** Investigation. **Gunnar M. Brown:** Investigation, Writing – review & editing. **Peter C. Burns:** Resources, Writing – review & editing. **Scott Carmichael:** Investigation, Writing – review & editing. **Lauren K. Callahan:** Investigation, Writing – review & editing. **Jes Koros:** Investigation. **Kevin Lee:** Investigation, Writing – review & editing. **Miriam Matney:** Investigation. **Anthony M. Miller:** Investigation, Writing – review & editing. **Orlando Olivas-Gomez:** Investigation. **Michael Paul:** Methodology, Resources, Writing – review & editing. **Richard Pardo:** Methodology. **Fabio Rivero:** Investigation. **Daniel Robertson:** Investigation, Writing – review & editing. **Ginger E. Sigmon:** Resources. **William W. von Seeger:** Investigation, Writing – review & editing. **Ed Stech:** Investigation, Methodology. **Regan Zite:** Investigation. **Philippe Collon:** Conceptualization, Funding acquisition, Methodology, Project administration, Supervision, Writing – review & editing.

Declaration of competing interest

The authors declare that they have no known competing financial interests or personal relationships that could have appeared to influence the work reported in this paper.

Data availability

Data will be made available on request.

Acknowledgements

We would like to thank Virginia Rodriguez for providing material from the St Anthony Mine in New Mexico. This work is supported by the National Science Foundation under Grant No. PHY-2011890 and the Nuclear Regulatory Commission award number 31310019M0037.

References

[1] S. Richter, A. Alonso, W. De Bolle, R. Wellum, P. Taylor, Isotopic "fingerprints" for natural uranium ore samples, Int. J. Mass Spectrom. 193 (1) (1999) 9–14.
[2] K. Wilcken, T. Barrows, L. Fifield, S. Tims, P. Steier, AMS of natural ^{236} U and ^{239} Pu produced in uranium ores, Nucl. Instrum. Methods B 259 (1) (2007) 727–732, accelerator Mass Spectrometry. 10.1016/j.nimb.2007.01.210.
[3] E. Browne, Nucl. Data Sheets 2579 (2006) 107.
[4] E. Browne, J.K. Tuli, Nucl. Data Sheets 751 (2013) 114.
[5] P. Steier, M. Bichler, L. Keith Fifield, R. Golser, W. Kutschera, F. Priller, S. Quinto, M.S. Richter, et al., Natural and anthropogenic ^{236}U in environmental samples, Nucl. Instrum. Methods B 266 (10) (2008) 2246–2250.
[6] K. Hain, P. Steier, M.B. Froehlich, R. Golser, X. Hou, J. Lachner, T. Nomura, J. Qiao, F. Quinto, A. Sakaguchi, ^{233}U/^{236}U signature al- lows to distinguish environmental emissions of civil nuclear industry from weapons fallout, Nat. Commun. 11 (1) (2020) 1275.
[7] E. Chamizo, M. Christl, M. López-Lora, N. Casacuberta, A. Wefing, T.C. Kenna, The potential of ^{233}U/^{236}U as a water mass tracer in the arctic ocean, J. Geophys. Res. Oceans 127 (3) (2022) n/a.
[8] A. Morereau, H. Jaegler, K. Hain, P. Steier, R. Golser, A. Beaumais, H. Lepage, F. Eyrolle, C. Grosbois, C. Cazala, A. Gourgiotis, Deciphering sources of U contamination using isotope ratio signatures in the Loire River sediments: Exploring the relevance of ^{233}U/^{236}U and stable Pb isotope ratios, Chemosphere (oxford) 307 (2022) 135658.
[9] E. Browne, J.K. Tuli, Nucl. Data Sheets 2657 (2008) 109.
[10] X.-L. Zhao, B. Francisco, W. Kieser, A. El-Jaby, C. Cochrane, I. Clark, A direct-AMS multi-isotope survey of uranium ore concentrates, Nucl. Instrum. Methods B 459 (2019) 98–114, https://doi.org/10.1016/j.nimb.2019.08.012.
[11] R. Edwards, C. Gallup, H. Cheng, Uranium-series Dating of Marine and Lacustrine Carbonates, Rev. Mineral. Geochem. 52 (1) (2003) 363–405. arXiv:https://pubs.geoscienceworld. org/msa/rimg/article-pdf/52/1/363/2943018/363.gsrmg.52.pdf, doi:10.2113/0520363. URL https://doi.org/10.2113/0520363.
[12] R.L. Edwards, K.B. Cutler, H. Cheng, C.D. Gallup, Geochemical evidence for quaternary sea-level changes, Treatise Geochem. 6 (2003) 625, https://doi.org/10.1016/B0-08-043751-6/06116-8.
[13] D. Berkovits, H. Feldstein, S. Ghelberg, A. Hershkowitz, E. Navon, M. Paul, ^{236}U in uranium minerals and standards, Nucl. Instrum. Methods B 172 (1) (2000) 372–376, 8th International Conference on Accelerator Mass Spectrometry. doi: https://doi.org/10.1016/S0168- 583X(00)00152- X.
[14] X.-L. Zhao, B. Francisco, Matrix-assisted production of actinide molecular anions for AMS, Nucl. Instrum. Methods B 510 (2022) 10–19.
[15] L. Fifield, Accelerator mass spectrometry of the actinides, Quat. Geochronol. 3 (3) (2008) 276–290.
[16] A.M. Clark, A.D. Nelson, T.L. Bailey, L.K. Callahan, A. Mazurek, P. Collon, Improvements for heavy-ion Accelerator Mass Spectrometry at the University of Notre Dame's Nuclear Science Laboratory, Nucl. Instrum. Methods Phys. Res. Sect. B: Beam Interact. Mater. Atoms 541 (2023) 342–349, https://doi.org/10.1016/j.nimb.2023.05.001.
[17] E. Browne, J.K. Tuli, Nucl. Data Sheets 108 (2007) 681–772.
[18] E.L. Garner, Standard reference materials: Uranium isotopic standard reference materials. (certification of uranium isotopic standard reference materials), U.S. Supt. of Docs. (1971).
[19] M. Christl, N. Casacuberta, J. Lachner, S. Maxeiner, C. Vockenhuber, H.-A. Synal, I. Goroncy, J. Herrmann, A. Daraoui, C. Walther, R. Michel, Status of ^{236}U analyses at ETH Zurich and the distribution of ^{236}U and ^{129}I in the North Sea in 2009, Nucl. Instrum. and Methods in Phys. Res. B 361 (2015) 510–516, the Thirteenth Accelerator Mass Spectrometry Conference. doi:https://doi.org/10.1016/j.nimb.2015.01.005. URL https://www.sciencedirect.com/science/article/pii/S0168583X1500018X.
[20] P. Steier, K. Hain, U. Klötzli, J. Lachner, A. Priller, S. Winkler, R. Golser, The actinide beamline at VERA, Nucl. Instrum. Methods Phys. Res. B 458 (2019) 82–89.
[21] M. De Cesare, N. De Cesare, A. D'Onofrio, L.K. Fifield, L. Gialanella, F. Terrasi, Mass and abundance ^{236}U sensitivities at CIRCE, Nucl. Instrum. and Methods in Phys. Res. B 361 (2015) 483–487.
[22] L. Zheng, H. Matsuzaki, T. Yamagata, ^{236}U accelerator mass spectrometry with a time-of-flight and energy detection system, Nucl. Eng. Technol. (2022).
[23] M. Srncik, K. Mayer, E. Hrnecek, M. Wallenius, Z. Varga, P. Steier, G. Wallner, Investigation of the ^{236}U/^{238}U isotope abundance ratio in uranium ores and yellow cake samples, Radiochimica Acta 99 (6) (2011) 335–339, https://doi.org/10.1524/ract.2011.1840.

[24] X.-L. Zhao, M.-J. Nadeau, L. Kilius, A. Litherland, The first detection of naturally-occurring ^{236}U with accelerator mass spectrometry, Nucl. Instrum. Methods B 92 (1) (1994) 249–253, https://doi.org/10.1016/0168- 583X(94)96014-3.
[25] D. Rokop, D. Metta, C. Stevens, $^{236}U/^{238}U$ measurements in three terrestrial minerals and one processed ore, Int. J. Mass Spectrom. 8 (4) (1972) 259–264.
[26] P.R. Fields, H. Diamond, D.N. Metta, D.J. Rokop, Airborne ^{236}U and its Effect on Lunar Sample Analysis, Internal Report (1976) 251–253.
[27] R.W. Williams, A.M. Gaffney, ^{230}Th-^{234}U model ages of some uranium standard reference materials, Proc. Radiochem. 1 (1) (2011) 31–35.
[28] G.R. Eppich, R.W. Williams, A.M. Gaffney, K.C. Schorzman, ^{235}U–^{231}Pa age dating of uranium materials for nuclear forensic investigations, J. Anal. At. Spectrom. 28 (5) (2013) 666.
[29] Z. Varga, A. Nicholl, E. Hrnecek, M. Wallenius, K. Mayer, Measurement of the $^{231}Pa/^{235}U$ ratio for the age determination of uranium materials, J. Radioanal. Nucl. Chem. 318 (3) (2018) 1565–1571.
[30] L.K. Fifield, A. Clacher, K. Morris, S. King, R. Cresswell, J. Day, F. Livens, Accelerator mass spectrometry of the planetary elements, Nucl. Instrum. Methods Phys. Res. B 123 (1–4) (1997) 400–404.
[31] M. Christl, L. Wacker, J. Lippold, H.-A. Synal, M. Suter, Protactinium-231: A new radionuclide for AMS, Nucl. Instrum. and Methods in Phys. Res. B 262 (2) (2007) 379–384. doi:https://doi.org/10.1016/j.nimb.2007.05.017.URL https://www.sciencedirect.com/science/article/pii/ S0168583X07011251.
[32] L. Wacker, E. Chamizo, L. Fifield, M. Stocker, M. Suter, H. Synal, Measurement of actinides on a compact AMS system working at 300kV, Nucl. Instrum. and Methods in Phys. Res. B 240 (1) (2005) 452–457, accelerators in Applied Research and Technology. doi:https://doi.org/10.1016/j.nimb.2005.06.144. URL https://www.sciencedirect.com/science/article/pii/ S0168583X05011158.
[33] E.E. Groopman, D.G. Willingham, A.J. Fahey, K.S. Grabowski, An overview of NRL's NAUTILUS: a combination SIMS-AMS for spatially resolved trace isotope analysis, J. Anal. At. Spectrom. 35 (3) (2020) 600–625, https://doi.org/10.1039/c9ja00344d.